Non-Destructive Characterization of Lightweight and Sustainble Rubber Modified Cementitious System

Shruti Singh[1], Hee-Jeong Kim[1,2], Tribikram Kundu[1,2,3]*

[1]Department of Civil and Architectural Engineering and Mechanics,
The University of Arizona, Tucson, USA
[2]Department of Materials Science and Engineering, University of Arizona, Tucson, USA
[3]Department of Aerospace and Mechanical Engineering, University of Arizona, Tucson, USA

ABSTRACT

Discarded rubber tires pose serious environmental challenges due to their non-biodegradability and accumulation in landfills; however, their elasticity, energy absorption capacity, and durability make them promising candidates for incorporation into cementitious systems, contributing to sustainable construction practices and end-of-life material utilization. Their mechanical performance is critical for durability and safety. However, incorporating recycled rubber fibers can alter both structural and acoustic properties, and conventional non-destructive testing techniques such as ultrasonic pulse velocity (UPV) may not fully capture microstructural damage. The relationship between nonlinear ultrasonic indicators and mechanical integrity in rubber-modified mortars remains unclear. Here we show that the Sideband Peak Count Index (SPCI), derived from frequency-domain analysis of ultrasonic signals, is highly sensitive to the internal damage caused by rubber fiber addition and correlates with compressive strength. Mortar specimens with 0–20% rubber fiber by volume were prepared and tested on the 7th day. The normalized SPCI value increased from 1.00 for the control specimen to a maximum value of 1.42 for 10% rubber, coinciding with the lowest compressive strength (11.91 MPa), and decreased to 0.98 for 20% rubber, reflecting microstructural reorganization and partial recovery of mechanical performance. These results demonstrate that SPCI effectively captures the nonlinear response of the mortar matrix and provides a quantitative, non-invasive tool for assessing strength loss and microcrack formation in fiber-modified cementitious system. These findings support the integration of nonlinear ultrasonic metrics into quality control and performance-based mix design for sustainable mortar and concrete applications.

Keywords**:** *Nondestructive testing, Ultrasonic Pulse Velocity, Non-linear Ultrasonic Testing, Rubberized Mortar, Sustainability*

1. INTRODUCTION

The global tire industry produces approximately 3 billion new tires annually, while simultaneously generating 800 million waste tires that require disposal [1]. This massive scale of tire production and disposal presents a profound environmental challenge, as discarded tires pose significant ecological threats through multiple pathways [2]. When improperly managed, tire stockpiles can ignite and burn for extended periods, releasing hazardous compounds including fine particulate matter (PM2.5), polycyclic aromatic hydrocarbons (PAHs), and heavy metals into the atmosphere [1][2]. Furthermore, tire wear particles generated during vehicle operation constitute the second-largest source of microplastic pollution globally, with an estimated 6 million metric tons released annually into the environment [3]. These particles, containing over 800 potentially toxic chemical compounds, have been linked to severe ecological impacts, including mass fish mortality events caused by substances such as 6PPD-quinone [1].

The integration of recycled tire rubber into concrete matrices offers remarkable acoustic damping properties, positioning it as an innovative solution for noise-sensitive applications [4]. Research demonstrates that crumb rubber concrete (CRC) exhibits superior sound absorption coefficients ranging from 0.30-0.70,

compared to conventional concrete values of 0.05-0.10 [5]. This enhanced acoustic performance stems from rubber's inherently high elastic modulus and energy dissipation characteristics, which facilitate efficient vibration damping and noise attenuation. Studies reveal that incorporating 50% crumb rubber can achieve up to 39% sound reduction, making rubberized concrete particularly valuable for highway noise barriers, building facades, and urban infrastructure where acoustic comfort is paramount [6][7].

Beyond acoustic benefits, incorporation of rubber particles into concrete substantially improves its thermal insulation properties, with thermal diffusivity decreasing by as much as 65.1% when 25% rubber content is used. This significant reduction means the composite material is much less responsive to rapid temperature changes when exposed to fluctuating thermal environments [8]. As a result, rubber-modified concrete acts as an effective thermal buffer, slowing the transfer of heat and helping to stabilize internal temperatures in pavements and buildings [9]. Such behavior is especially beneficial for sustainable construction, as it not only helps mitigate urban heat island effects but also reduces energy consumption for heating or cooling, positioning rubber-modified concrete as a valuable material for climate-resilient infrastructure. The synergistic combination of lightweight characteristics and improved thermal performance positions rubber-modified concrete as a sustainable alternative for multiple applications where thermal management and density reduction are critical design considerations [7][10].

The utilization of waste tire rubber in sustainable concrete formulations represents a paradigmatic shift toward circular economy principles in construction materials [11]. Contemporary research demonstrates that properly treated rubber particles can achieve compressive strengths within 10-15% of control mixtures while providing substantial environmental benefits through waste stream diversion [6]. Advanced surface treatment protocols, including sodium hydroxide modification and cement coating techniques, have shown remarkable success in improving rubber-cement interfacial bonding, with strength enhancements of up to 83.5% reported in recent investigations [12]. These developments support the viability of rubberized concrete for structural and semi-structural applications where performance optimization balances mechanical requirements with sustainability objectives.

Nonlinear non-destructive testing (NDT) techniques offer significant advantages over conventional linear methods for characterizing complex composite materials such as rubber-modified concrete [13][14]. Unlike traditional ultrasonic pulse velocity (UPV) measurements that rely solely on wave velocity information, nonlinear NDT approaches exploit harmonic generation and nonlinear wave scattering phenomena to detect microstructural changes with superior sensitivity [15]. Advanced ultrasonic techniques such as higher harmonic generation and sideband analysis provide early warning capabilities for damage initiation and progression, enabling proactive maintenance strategies that extend infrastructure service life [16][17]. The enhanced sensitivity of nonlinear methods stems from their ability to detect distributed damage, microcracks, and interfacial debonding at stress levels well below those required for linear method-based detection techniques [18].

The Sideband Peak Count Index (SPCI) emerges as a particularly powerful parameter for microstructural damage assessment, offering superior diagnostic capabilities compared to conventional UPV measurements. Recent investigations demonstrate that SPCI effectively capture the transition from damage-dominated scattering to structural consolidation in heterogeneous materials, providing quantitative metrics for internal damage states and interfacial integrity [19]. This technique exhibits exceptional sensitivity to early-stage deterioration mechanisms, including interfacial transition zone modifications, microcrack development, and pore structure evolution [20]. The ability of SPCI to monitor damage progression in real-time positions it as an invaluable tool for quality control and performance prediction in sustainable concrete applications [21].

Despite the promising characteristics of rubber-modified concrete, significant research gaps persist in comprehensive characterization methodologies for these innovative materials. Current literature lacks systematic investigations integrating mechanical performance, durability assessment, and advanced NDT characterization for rubberized concrete systems. Most existing studies focus on isolated properties or employ conventional testing approaches that fail to capture the complex microstructural interactions governing performance in these heterogeneous composite systems [23]. The absence of standardized protocols for nonlinear NDT evaluation of rubber-modified concrete

represents a critical knowledge gap that limits practical implementation and performance-based specification development.

The development of advanced NDT methodologies specifically tailored for sustainable cementitious materials represent an urgent research priority in infrastructure engineering. Conventional assessment techniques prove inadequate for evaluating innovative composite materials where interfacial characteristics and microstructural organization govern performance. Modern infrastructure engineering requires rapid, accurate, and non-invasive evaluation methods that can assess both structural integrity and long-term durability characteristics without disrupting service operations. The integration of artificial intelligence and machine learning approaches with advanced NDT techniques offers promising avenues for developing comprehensive material characterization frameworks.

This investigation addresses the identified knowledge gaps by presenting a comprehensive study integrating mechanical testing, advanced nonlinear NDT characterization, and microstructural analysis of rubber tire mulch-modified concrete for sustainable applications. The research employs a systematic approach combining compressive strength evaluation, ultrasonic pulse velocity assessment, Sideband Peak Count Index analysis, and scanning electron microscopy to establish correlations between microstructural characteristics and performance parameters. By developing relationships between conventional and advanced NDT techniques, this work provides essential foundations for performance-based specifications and quality control protocols for sustainable construction utilizing recycled tire materials. The findings contribute to the broader objectives of infrastructure sustainability while advancing the scientific understanding of composite material characterization through innovative non-destructive evaluation methodologies.

2. MATERIALS AND METHODOLOGY

2.1. Materials

The materials utilized for the preparation of the test specimens consisted of cement, water, fine aggregate, and recycled rubber tire mulch. Potable tap water, compliant with ASTM C1602/C1602M-22 [24], was used exclusively for mixing the specimens. The water was free of harmful substances such as oils, acids, alkalis, and organic contaminants that could negatively impact hydration. A uniform water-to-cement (w/c) ratio was maintained across all batches to ensure consistency in mechanical and NDT evaluations. Specimens were not water-cured; instead, they were stored in controlled laboratory conditions and allowed to harden under sealed/ambient curing.

The binder employed in this investigation was Type I/II Portland cement, conforming to the specifications outlined in ASTM C150/C150M-22 [25]. This dual classification ensures the cement satisfies the requirements of both Type I and Type II categories, making it suitable for conventional construction applications while also providing resistance to environments with moderate sulfate exposure. Such versatility renders it an effective option for concrete exposed to variable soil and groundwater conditions. The cement was stored in sealed containers to prevent premature hydration or contamination from ambient moisture. Laboratory characterization confirmed a specific gravity of 3.15 and a Blaine fineness of roughly 350 m^2/kg, values consistent with industry standards.

Natural river sand was selected as the fine aggregate, meeting the grading and durability criteria prescribed by ASTM C33/C33M-18 [26]. Prior to use, the material was oven-dried and sieved through a 4.75 mm (No. 4) sieve to remove oversized particles and ensure uniformity in the matrix. The physical properties of the sand were determined according to ASTM C128-22 [27], with results showing a specific gravity of 2.57 and a water absorption of 0.77%. The moisture content, measured using ASTM C566-19 [28], was found to be 0.129%. These parameters were incorporated into the mix proportioning process to accurately regulate the effective water-to-cement ratio.

Fig: 1 Rubber Tire Mulch.

The rubber tire fibers used in this study were sourced from Vigoro® 100% Recycled Premium Rubber Mulch, a commercially available product derived

from post-consumer vehicle tires. The as-received material consisted of irregularly shaped particles with considerable variation in size and geometry. To ensure uniformity and suitability for mortar mixing, the mulch was manually processed by sorting and cutting into fibrous strips using hand tools. The resulting fibers measured approximately 10–20 mm in length and 1–3 mm in width. This size range was selected based on preliminary trial mixes, which indicated a balance between improved workability and potential reinforcement efficiency in mortar applications. The physical characterization of the rubber fibers included the determination of specific gravity, which was performed in accordance with ASTM D6270 – Standard Practice for Use of Scrap Tires in Civil Engineering Applications [29]. The specific gravity of the processed fibers was found to be 0.80, significantly lower than that of mineral aggregates. This lower density was considered in the adjustment of mix proportions and water demand, and it also provided an indication of the potential influence of rubber inclusion on the overall density and mechanical properties of the mortar matrix.

2.2. Mix Design

The mortar mixtures for this study were developed following the procedures outlined in ASTM C305-20 – Standard Practice for Mechanical Mixing of Hydraulic Cement Pastes and Mortars of Plastic Consistency [30] and ASTM C109/C109M-21 – Standard Test Method for Compressive Strength of Hydraulic Cement Mortars [31]. The primary objective was to investigate the influence of recycled rubber tire fibers on the mechanical and non-destructive properties of cementitious mortar. A target mean compressive strength exceeding 40 MPa at 28 days was selected, and a water-to-cement (w/c) ratio of 0.432 was maintained across all mixtures to ensure consistent workability and hydration. The cement-to-fine aggregate (C/F) ratio was kept constant at 0.68 to maintain uniform binder-to-aggregate proportions.

Five mortar mixtures were prepared: one control mixture without rubber (TF_00) and four mixtures incorporating 5%, 10%, 15%, and 20% rubber fiber by volume, designated as TF_05, TF_10, TF_15, and TF_20, respectively. Unlike partial replacement studies, the rubber fibers were introduced as a fiber additive, while the quantities of water, cement, and sand were held constants for all mixes.

Table 1 presents the mixture proportions, where the rubber fiber content ranged from 0 to 186.667 kg/m³ depending on the volumetric percentage. The constant binder, aggregate, and water contents (896.533 kg/m³ OPC, 1316 kg/m³ sand, and 387.467 kg/m³ water) ensured that the variations in properties could be attributed solely to the addition of rubber fibers. The specific gravity and water absorption of the rubber fibers, determined in accordance with ASTM D6270 – Standard Practice for Use of Scrap Tires in Civil Engineering Applications [29], were accounted for in the mix design to maintain the effective water-to-cement ratio and optimize workability.

Table 1: Mortar mix proportions for control and rubber-fiber-modified mixtures

Sample ID	Water (kg/m³)	OPC (kg/m³)	Sand (kg/m³)	Rubber (kg/m³)	w/c (mass)
TF_00	387.467	896.533	1316.000	0.000	0.432
TF_05	387.467	896.533	1316.000	46.667	0.432
TF_10	387.467	896.533	1316.000	93.333	0.432
TF_15	387.467	896.533	1316.000	140.000	0.432
TF_20	387.467	896.533	1316.000	186.667	0.432

This design approach enabled a systematic evaluation of the impact of increasing rubber fiber content on mortar density, compressive strength, and non-destructive testing responses, while minimizing confounding effects from changes in water, cement, or aggregate content.

2.3. Specimen preparation

The mortar specimens were prepared following the procedures specified in ASTM C305-20 – Standard Practice for Mechanical Mixing of Hydraulic Cement Pastes and Mortars of Plastic Consistency [30]. All constituents, cement, fine aggregate, water, and rubber fibers, were preconditioned under saturated surface-dry (SSD) conditions to ensure consistent moisture content and to prevent unintended absorption during mixing.

Mechanical mixing was performed using a standardized mixer equipped with a flat beater paddle and stainless-steel bowl. Initially, the dry components (cement and fine aggregate) were mixed at low speed (140 ± 5 rpm) for 30 seconds to achieve a uniform distribution. The pre-measured water was then added gradually over 30 seconds while mixing continued at the same speed. The mixture was subsequently mixed at medium speed (285 ± 10 rpm) for 30 seconds. A 90-second rest period followed, during which any material adhering to the

bowl sides was scraped down. Mixing then resumed at medium speed for an additional 60 seconds. Rubber fibers were incorporated manually immediately after the rest period and blended into the mortar during the final mixing stage to ensure homogeneous dispersion. The total mixing procedure adhered to ASTM C305 [30] guidelines, resulting in a consistent and workable mortar suitable for casting.

Specimens were cast in molds of 50 mm × 50 mm × 50 mm cubes, following ASTM C109/C109M-21 [31], Prior to casting, the interior surfaces of all molds were coated with a thin layer of mineral oil to prevent adhesion. The mortar was placed in two equal layers, with each layer compacted on a vibrating table for approximately 30 seconds to eliminate entrapped air and ensure uniform material distribution. The top surface of each specimen was then finished with a trowel to produce a smooth, level surface.

Immediately after casting, the specimens were covered with a plastic sheet and allowed to rest at room temperature for 24 hours to minimize moisture loss and facilitate initial setting. Following demolding, all specimens were transferred to a controlled air-curing environment maintained at 23 ± 2°C and approximately 50% relative humidity. The curing procedure was adapted from ASTM C192/C192M-22 [32] to reflect air-curing conditions. Specimens were cured for 7 days prior to testing. Throughout the curing period, environmental conditions were carefully monitored to ensure uniform hydration, prevent surface drying, and avoid cracking or direct exposure to sunlight or strong airflow.

2.4. Testing Method

2.4.1. Scanning Electron Microscope Analysis

Fractured specimens were subjected to microstructural characterization using a Tescan Mira3 scanning electron microscope (SEM). Prior to imaging, all samples were oven-dried to remove residual moisture. To enhance surface conductivity, a thin gold coating of approximately 5 nm was applied to the fracture surfaces employing an automated sputter coater. SEM imaging was performed in secondary electron mode with an accelerating voltage of 15 kV, and a working distance of 10 mm. Micrographs were acquired to investigate fracture morphology and relevant surface features.

2.4.2. Compression Test

The compressive strength of the mortar specimens was determined in accordance with the procedures outlined in ASTM C109/C109M-21 – Standard Test Method for Compressive Strength of Hydraulic Cement Mortars [31] (Using 2-in. or [50-mm] Cube Specimens). The primary objective of this test was to evaluate the influence of rubber fiber incorporation on the load-bearing capacity of the mortar.

Cube specimens measuring 50 mm × 50 mm × 50 mm were used for all strength evaluations. Following casting, the specimens were demolded after 24 hours and subsequently subjected to controlled air curing at 23 ± 2 °C and 50% relative humidity until the designated age of testing. Compressive strength tests were carried out on the 7th day, to check the early-age performance of the mixtures.

Prior to testing, each specimen was carefully examined to ensure it was free from visible surface cracks, edge defects, or signs of improper compaction, as such imperfections could introduce variability in test results. The specimens were then centrally aligned between the platens of a calibrated compression testing machine with a capacity suitable for anticipated failure loads. Proper alignment was verified to ensure uniform load distribution across the specimen cross-section and to prevent eccentric loading effects.

The load was applied continuously and without shock at a controlled rate of 1.5 ± 0.5 MPa/s, as prescribed by ASTM C109/C109M-21 [31]. Loading was continued until visible cracking and ultimate failure of the specimen occurred. The maximum applied load at failure was recorded, and the compressive strength was computed using the following relation:

$$f_c = \frac{P}{A}$$

where:

fc = compressive strength (MPa)

P = maximum applied load at failure (N)

A = cross-sectional area of the specimen (mm^2)

For each mixture, the results were averaged from three replicate specimens, and the mean compressive strength was reported. The use of multiple replicates minimized

experimental variability and ensured the reliability and reproducibility of the results. Standard deviations were also calculated to quantify the degree of scatter in the measured data.

This systematic testing protocol provided a robust evaluation of the compressive behavior of mortar mixtures containing varying proportions of rubber fibers, thereby enabling direct comparison with the control mix.

2.4.3. Linear Ultrasonic Testing

The ultrasonic pulse velocity (UPV) method was employed to evaluate the internal quality of the mortar mixtures in accordance with ASTM C597 – Standard Test Method for Pulse Velocity Through Concrete [33]. This nondestructive technique was selected to investigate the influence of recycled rubber fiber addition on the stiffness and integrity of the mortar matrix.

All measurements were performed on 50 mm cube specimens, consistent with the geometry used for compressive strength testing. Although ASTM C597 [33] recommends a minimum path length of approximately 50 mm for accurate transit-time measurement, the cube geometry in this study provided the shortest permissible path length. While the absolute UPV values obtained from 50 mm cubes may not directly align with the standard quality classifications, the use of identical specimen geometry and consistent test setup across all mixtures ensured that any systematic deviations were uniform. Thus, the UPV data are considered reliable for relative performance comparisons and for assessing the effect of rubber incorporation on microstructural integrity.

Testing was conducted using a commercial UPV device equipped with 54 kHz transducers arranged in a direct transmission configuration, where the transmitting and receiving transducers were placed on opposing cube faces. A thin layer of petroleum-based coupling gel was applied at the transducer–specimen interface to improve acoustic coupling and minimize signal loss due to surface roughness. Prior to each measurement session, the instrument was calibrated against a standard reference bar supplied by the manufacturer to ensure accuracy.

UPV testing was performed on the 7th day for all mixtures. For each specimen, three independent measurements were taken, and the average pulse velocity was calculated to account for experimental variability.

The pulse velocity (V) was determined as:

$$V = \frac{L}{T}$$

where:

V = ultrasonic pulse velocity (m/s),

L = path length, equal to the cube dimension,

T = measured travel time of the ultrasonic pulse (s).

The mean velocity for each specimen was obtained as:

$$\overline{V} = \frac{1}{n}\sum_{i=1}^{n} V_i$$

where is the number of replicate measurements.

2.4.4. Non-Linear Ultrasonic Testing

Nonlinear ultrasonic testing was conducted on the mortar specimens on the 7th day of curing, encompassing both reference samples and specimens incorporating varying proportions of rubber tire fibers. The primary objective of this investigation was to assess the influence of rubber fiber incorporation on the nonlinear elastic behavior of the mortar matrix through frequency-domain analysis.

The nonlinear ultrasonic response was evaluated using lead zirconate titanate (PZT) transducers in a transmission configuration. Two PZTs were positioned on opposite smooth faces of each 50 mm cube specimen, with one transducer serving as the transmitter and the other one as the receiver. To ensure optimal wave transmission and minimize interfacial impedance, a thin layer of petroleum jelly was applied at the transducer–specimen interface to eliminate potential air gaps.

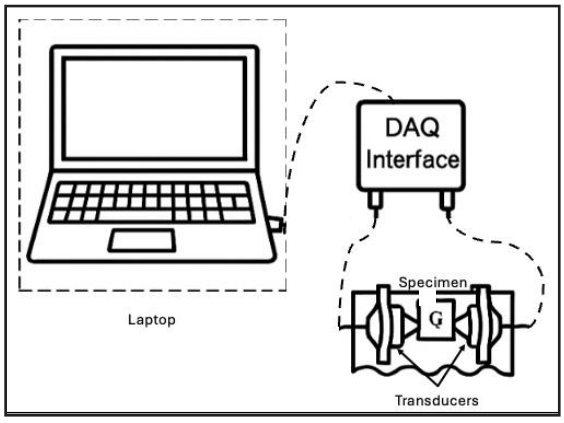

Fig. 2: Schematic of Experimental Setup

The excitation signal consisted of a sinusoidal input pulse at a fundamental frequency of 42.5 kHz, chosen to induce measurable scattering effects within the cementitious matrix and capture the evolution of nonlinear material behavior associated with fiber inclusion. The acquired signals were sampled at 50 MHz using a high-speed digital oscilloscope, and a post-trigger silent period of 3000 µs was employed to guarantee complete capture of the transient response. To reduce the influence of random noise and enhance signal fidelity, each measurement was averaged over 128 repeated acquisitions.

Signal preprocessing involved the application of a Hann windowing function, which mitigates spectral leakage, reduces boundary discontinuities, and improves the resolution of harmonic and sideband components in the frequency domain [34][35]. This approach enhances the ability to isolate weak higher-order harmonics from the dominant fundamental frequency, thereby increasing sensitivity to subtle nonlinearities in the mortar matrix. Prior to analysis, the transient signals were normalized to their peak amplitude to ensure comparability across specimens with differing material compositions.

The experimental apparatus comprised of a computer-controlled data acquisition system, integrating an arbitrary waveform generator, a high-speed oscilloscope, and a data logger (Figure 2). The actuator PZT was connected to the waveform generator output, while the receiver PZT was interfaced with the oscilloscope input, enabling synchronous acquisition of transmitted signals.

Post-processing of the acquired signals was performed in both time and frequency domains to extract relevant nonlinear features. The nonlinear response of each specimen was quantified using the Sideband Peak Count Index (SPCI), a metric designed to capture sideband generation arising from microcracks, pore formation, and matrix modifications induced by the incorporation of rubber fibers. Initially, the transient signals were transformed into spectral representations using Fast Fourier Transform (FFT) (Figure 3). Subsequently, a threshold window ranging from 0.1% to 3% of the peak amplitude was established for each specimen. A variable threshold line was then scanned across this range, and the corresponding sideband peaks exceeding the threshold were enumerated. The resulting plot of threshold versus sideband peak count provided a systematic evaluation of nonlinear contributions, and the average number of peaks across the threshold range was reported as the final SPCI value for each specimen.

This methodology enabled a robust, quantitative assessment of nonlinear ultrasonic behavior, providing insights into the microstructural interactions and matrix modifications induced by the inclusion of rubber fibers within the cementitious mortar system.

2.4.5. Density

The density of the mortar specimens was evaluated to quantify the influence of rubber tire incorporation on the lightweight characteristics of the mixtures and to classify the material according to established lightweight concrete criteria. Hardened mortar density was measured on 50 mm cube specimens at 28 days following ASTM C642, Standard Test Method for Density, Absorption, and Voids in Hardened Concrete [36]. Specimens were first surface-dried and weighed, then oven-dried at 110 ± 5°C until consecutive weighing's differed by less than 0.5% over 24-hour intervals to obtain the oven-dry mass. The specimens were subsequently immersed in tap water at 23 ± 2°C for a minimum of 48 hours until mass

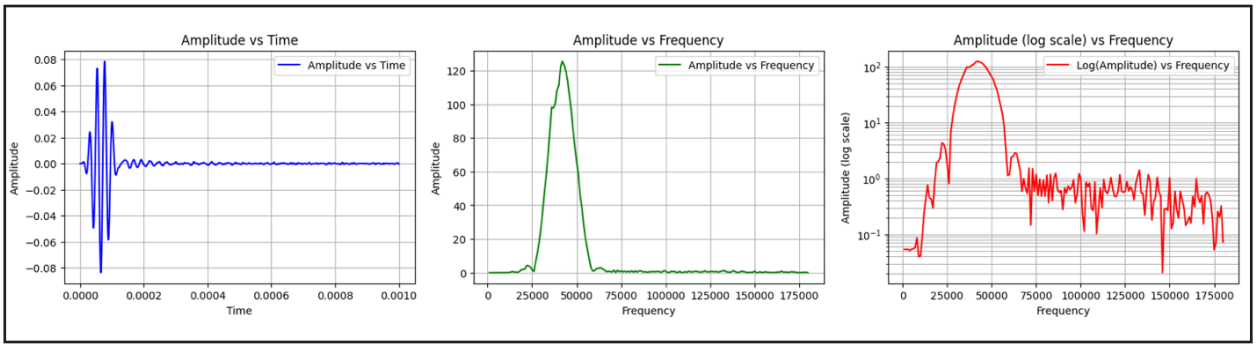

Fig. 3: Transient signal (left figure) and Spectral Plots in normal scale (middle figure) and log-normal scale (right figure) after FFT

stabilization, after which the saturated surface-dry mass was determined. The apparent mass of each specimen when suspended in water was also recorded. Using these measurements, bulk density (dry) was calculated using standard formulations, with the density of water at 1000 kg/m³ as a reference. All measurements were performed in triplicate to ensure statistical reliability. This systematic density characterization provides a robust evaluation of the lightweight nature of rubber-modified mortar, offering critical data for both structural design and sustainability assessments.

3. RESULTS AND DISCUSSION

3.1. Scanning Electron Microscope

Scanning electron microscopy (SEM) analysis provided valuable insights into the microstructural characteristics of the rubber-modified mortar, particularly at the interface between the rubber particles and the cementitious matrix. The micrographs revealed distinct separation between the rubber particles and the surrounding matrix, which directly correlates with the reduction in compressive strength due to the inherently weak rubber–cement bonding. Despite this debonding tendency, the presence of hydration products adhering to the rubber surface (Fig. 4) indicates partial interaction between the rubber and the cementitious phase, suggesting that some degree of chemical or physical adhesion occurs even in these hydrophobic systems.

Previous studies have reported the formation of hydration products on the rubber surface, confirming that limited interaction between rubber particles and cement hydrates can occur at the interface [37,38]. These studies observed characteristic elemental peaks of calcium (Ca), silicon (Si), and oxygen (O) near rubber inclusions, along with increased carbon and sulfur from the rubber itself, suggesting the coexistence of hydration compounds and polymer residues at the contact zone.

The morphological continuity observed in the present SEM images supports this interpretation, implying that such localized adhesion may contribute to the overall integrity of the matrix even at higher rubber contents. The hydrophobic nature of rubber was also found to influence the local hydration process, promoting preferential water migration pathways during curing and leading to incomplete hydration zones near the particle surfaces. This effect was particularly evident in specimens with higher rubber replacement, where SEM micrographs showed extensive microcracking radiating outward from the particle boundaries. These cracks are likely to serve as stress concentrators, promoting early failure under compressive loading, as frequently reported in polymer-modified cementitious systems.

Interestingly, while increased rubber incorporation compromised the compressive strength, the retained microstructural integrity at higher rubber contents suggests a modified fracture behavior. The transition from a brittle to a quasi-ductile failure mode, attributable to the crack-arresting and energy-absorbing capacity of the rubber particles, is evident in the SEM observations.

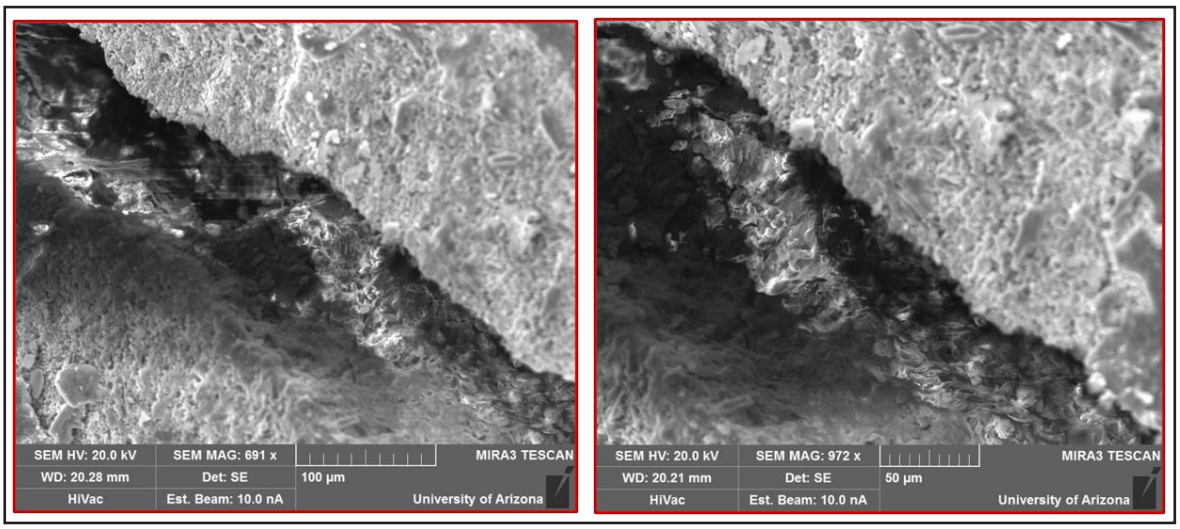

Fig. 4: SEM micrograph of rubber-modified mortar at 100 µm and 50 µm

3.2. Compression Test

The compressive strength results of rubber-modified mortar mixtures exhibited a distinctly non-linear response, with an initial sharp reduction in strength at low replacement levels followed by partial recovery as the rubber content increased. The control mixture (TF_00) achieved an average compressive strength of 37.41 MPa. At 5% rubber replacement (TF_05), the strength decreased dramatically to 18.07 MPa, corresponding to a reduction of 51.7%. A further decline was observed at 10% replacement (TF_10), which yielded the lowest strength in the series (11.91 MPa), representing a 68.2% reduction relative to the control (Figure 5). This pronounced degradation at low replacement levels is attributed to the hydrophobic nature of rubber surfaces which hinders chemical bonding with the cement matrix and promotes preferential water migration during hydration, resulting in incomplete hydration halos adjacent to the rubber inclusions. In addition, the large elastic modulus mismatch between rubber (1–2 GPa) and the surrounding cement paste (25–35 GPa) introduces stress concentration effects, encouraging crack initiation at the rubber – matrix interface under compressive loading.

A reversal of this downward trend was noted beyond 10% replacement, where strength increased from 11.91 MPa at TF_10 to 15.69 MPa at TF_15, marking a 31.7% recovery. This improvement suggests the presence of critical threshold effects where the role of rubber in the matrix transitions from being predominantly detrimental to partially beneficial. At intermediate replacement levels, rubber particles may contribute to improved packing density by filling interstitial voids between larger aggregate grains, leading to localized densification of the matrix. The more refined particle size distribution reduces overall porosity, which may partially offset the weakness of the bond between rubber and cementitious matrix. Additionally, the distribution of rubber particles appears to support limited crack-bridging behavior. Microstructural observations indicate that rubber inclusions can impede crack propagation by providing energy-dissipating pathways, which in turn explains the quasi-ductile behavior reported in similar systems.

At higher replacement levels, a further stabilization was observed, with compressive strength increasing from 15.69 MPa (TF_15) to 16.61 MPa (TF_20), a 5.9% improvement. This recovery, though modest, suggests that compensatory mechanisms become more pronounced at elevated rubber contents. SEM imaging of selected samples confirmed localized formation of hydrate at certain rubber–cement interfaces, demonstrating that partial interfacial bonding does occur despite the hydrophobic surface chemistry of rubber. Approximately 15–20% of examined interfaces exhibited such features, indicating limited but meaningful chemical interactions. Furthermore, higher rubber concentrations likely promote stress redistribution within the matrix, as clusters of flexible particles form semi-continuous phases that mitigate localized stress concentrations and delay catastrophic crack propagation.

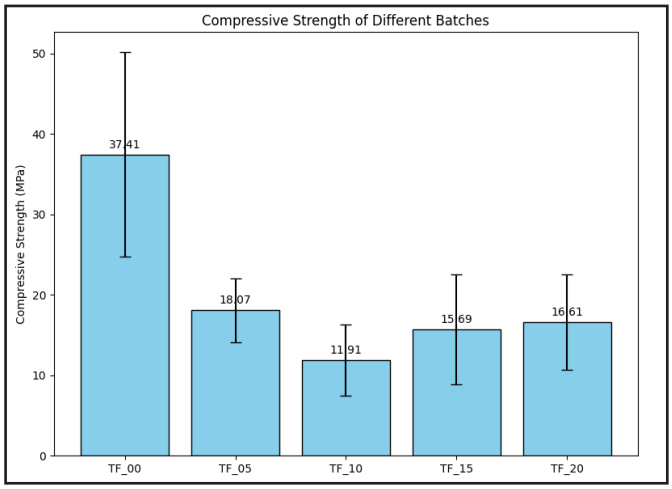

Fig. 5: Compressive Strength on 7th day

The overall compressive strength behavior therefore reflects a competition between interfacial weakening, which dominates at low replacement levels, and packing efficiency and stress redistribution effects, which begin to exert influence at moderate to high replacement levels. While the strength values at 20% replacement remain below that of the control mixture, the stabilization of compressive strength at higher rubber contents highlights the potential for performance optimization. Importantly, the transition from brittle failure in the control and low replacement mixtures to quasi-ductile behavior at higher rubber contents suggests added benefits in terms of post-peak load-bearing capacity. This characteristic is particularly relevant for structural applications where cyclic loading and energy absorption are critical performance requirements.

The findings emphasize that compressive strength in rubber-modified concretes cannot be evaluated in isolation. Although the absolute strength is reduced, the

observed non-linear development pattern suggests the existence of optimal replacement levels, likely in the range of 15–20%, where the detrimental effects of weak bonding between rubber and cementitious matrix are partially balanced by microstructural and mechanical advantages. These results provide an experimental basis for pursuing performance-based mix designs in which strength, ductility, and sustainability are considered simultaneously.

3.3. Ultrasonic Pulse Velocity

The ultrasonic pulse velocity (UPV) measurements on the 7th day revealed systematic variations in wave propagation characteristics as a function of rubber tire mulch content. The control mixture (TF_00) achieved the highest velocity of 3805 m/s, providing the baseline for conventional mortar. With the introduction of rubber, a gradual reduction in UPV was observed: TF_05 recorded 3775 m/s, TF_10 measured 3762 m/s, and TF_15 reached the lowest value of 3681 m/s. This steady decline, amounting to a 3.26% reduction from the control to TF_15, indicates the progressive impact of rubber incorporation on acoustic performance (Figure 6). Rubber's significantly lower elastic modulus contributes to reduced wave velocity by lowering the composite stiffness, while incomplete hydration halos and interfacial microcracks identified through SEM act as additional scattering sites. The acoustic impedance mismatch between the low-stiffness rubber particles and the surrounding cementitious matrix also gives rise to scattering, reflection, and attenuation of the transmitted ultrasonic waves.

Interestingly, at 20% replacement (TF_20), a recovery in UPV was recorded, with the velocity increasing to 3704 m/s. This finding diverges from the otherwise monotonic decline and suggests compensatory mechanisms at higher replacement levels. Improved particle packing and reduced void content at elevated rubber concentrations may enhance the continuity of the propagation path, partially offsetting interfacial scattering effects. The possibility of localized bonding improvements, such as the formation of C–S–H gels bridging rubber–cement interfaces observed in SEM images, may also contribute to maintaining acoustic connectivity within the matrix. Together, these factors provide a plausible explanation for the modest recovery in velocity at TF_20.

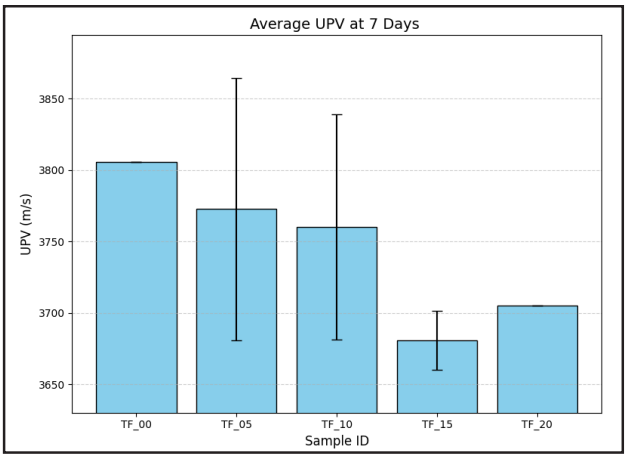

Fig. 6: Ultrasonic Pulse Velocity on the 7th Day

In terms of quality classification, the UPV values place the control and 5% replacement mixtures in the "good" category, while 10–20% replacements fall within the upper range of "doubtful" quality according to IS 13311-1:1992 and BS 1881 standards. Despite this downward shift, the narrow overall range of velocities (3681–3805 m/s) indicates that the incorporation of rubber does not critically compromise the material's structural integrity. Error analysis confirmed good repeatability, with coefficients of variation below 5% across all mixtures. The slightly higher scatter observed for TF_05 and TF_10 suggests transitional microstructural states where rubber distribution exerts greater influence on wave propagation.

The results highlight that UPV trends in rubber-modified concrete are governed by a competition between weakening mechanisms, dominated by elastic modulus reduction and interface scattering at low contents, and compensatory effects such as packing density and stress redistribution at higher contents. The observed recovery at 20% replacement reinforces this balance, suggesting that critical thresholds exist where structural organization improves despite the intrinsic weakness of the rubber–cement interface. Overall, the UPV analysis provides meaningful insights into the internal structure of rubber-modified mortar, confirming that although quality classification is reduced compared to conventional mixes, the measured values remain within acceptable ranges for sustainable construction applications.

3.4. Sideband Peak Count Index (SPCI)

The normalized Sideband Peak Count Index (SPCI) revealed a distinct non-linear trend with increasing

rubber tire mulch content (Figure 7). Normalizing all SPCI values with respect to that of the control mixture (TF_00 = 1.00) it is found that SPCI rose to 1.24 for 5% replacement and reached its maximum value of 1.42 for the 10% replacement, followed by a decline to 1.14 and 0.98 for 15% and 20% replacements, respectively.

The initial rise in SPCI at 5% and 10% rubber content reflects enhanced microcrack development and interfacial voids at the rubber–cement boundaries. The maximum SPCI value for TF_10 coincided with the lowest compressive strength (11.91 MPa) confirming the disruption of acoustic continuity and mechanical integrity at these replacement levels.

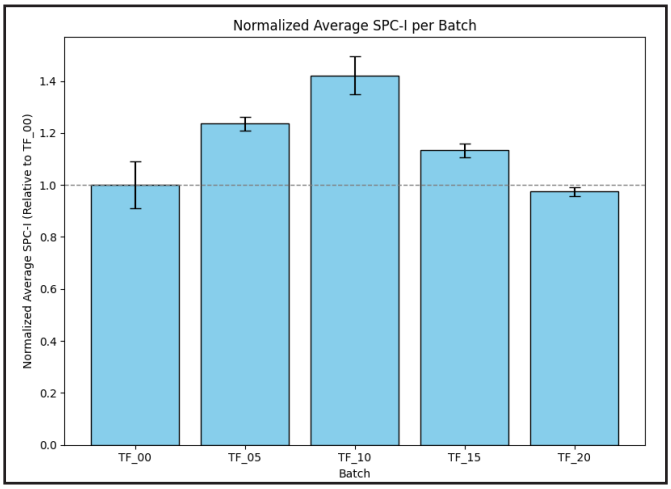

Fig. 7: Average Sideband Peak Count Index on the 7th day

Beyond 10% replacement, the SPCI values began to decline, indicating a shift in the governing microstructural processes. At higher rubber contents, particle redistribution and improved packing density appear to reduce micro-cracks or micro-discontinuities between rubber and mortar. Localized C–S–H gel bridging at rubber–cement interfaces contributes to enhanced connectivity, partially restoring both compressive strength (15.69 MPa and 16.61 MPa for TF_15 and TF_20) and UPV (3681 m/s and 3704 m/s).

These observations demonstrate that SPCI is highly sensitive to the competing effects of microstructural damage and reorganization in rubber-modified concrete. It is interesting to note that the variation of SPCI and compressive strength follow exactly opposite trends. SPCI first goes up and then goes down while compressive strength first goes down and then goes up. UPV also first goes down and then goes up. However, the minimum values of UPV and compressive strength are not observed for the same specimen while the maximum value of SPCI and the minimum value of compressive strength are observed for the same specimen.

The maximum SPCI value indicating largest density of microcracking for TF_10 specimen giving rise to the minimum strength of the specimen makes perfect sense. Thus, in this example in comparison to the UPV, the SPCI appears to be a better indicator of the specimen strength variation trend.

In particular, the ability of SPCI to capture the transition from damage-dominated scattering at moderate replacement levels to structural consolidation at higher rubber contents highlights its potential as a diagnostic tool for quality control in sustainable applications.

3.5. Density

The hardened density of the 50 mm cube specimens showed a consistent decrease with increasing rubber tire mulch content. The control mixture (TF_00) recorded the maximum oven-dry density of 2274.7 kg/m³, which progressively reduced to 2272.0 kg/m³ (TF_05), 2224.0 kg/m³ (TF_10), 2205.3 kg/m³ (TF_15), and 2170.7 kg/m³ (TF_20). Although all mixtures remained within the normal-weight classification range of 2000–2400 kg/m³ as defined by ASTM C567/C567M, the overall reduction of 4.6% from TF_00 to TF_20 highlights the effectiveness of rubber incorporation in achieving mass reduction (Figure 8).

The density decrease is directly linked to the low specific gravity of rubber (0.8 g/cm³) compared with natural sand (2.65 g/cm³). The volumetric replacement of fine aggregate with rubber particles lowers the bulk unit weight of the mixtures, in line with the absolute volume design principle.

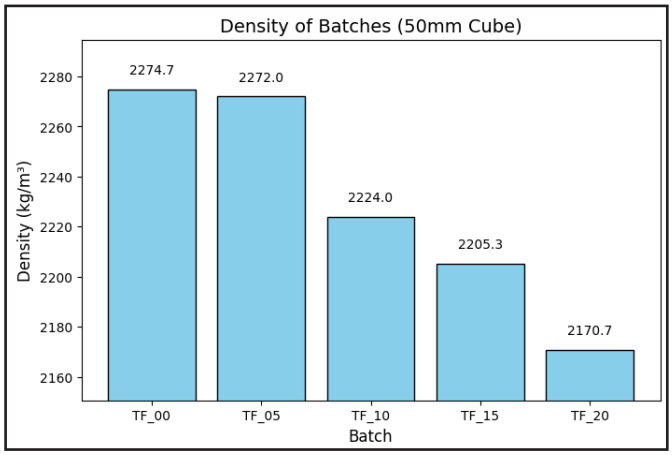

Fig. 8: Average Density of Rubberized Concrete

The most significant density loss occurred between TF_05 and TF_10 (−2.1%), which also corresponded to the maximum reduction in compressive strength (68.2%) and a notable decline in UPV. This suggests a critical threshold at 10% replacement, beyond which the matrix experiences marked increases in porosity and deterioration of interfacial bonding. Further increases in rubber content continued to reduce density, but at a slower rate (−1.7% from TF_10 to TF_20). Interestingly, compressive strength and UPV showed partial recovery in this range, indicating that microstructural reorganization and improved particle packing at higher rubber dosages may mitigate some of the adverse effects of density reduction on stiffness and integrity.

From an application standpoint, the measured reductions in density indicate the potential of rubberized concrete for lightweight pavement related and semi-structural applications. The decrease in dead load can ease foundation demands and provide additional benefits such as improved thermal insulation. However, the trade-off with strength and stiffness necessitates careful optimization of rubber content to balance structural performance with mass savings.

4. CONCLUSION

This study evaluated the influence of recycled rubber tire mulch on the mechanical, physical, and non-destructive characteristics of cementitious mortar designed for pavement applications. The results highlight a complex, non-linear response of the composite system to incremental rubber incorporation.

- Compressive strength exhibited a sharp reduction from 37.4 MPa in the control mix to 11.9 MPa at 10% replacement (−68%), followed by partial recovery to 16.6 MPa at 20%. Ultrasonic pulse velocity showed a similar trend, declining from 3805 m/s in the control to 3681 m/s at 15% replacement, then rebounding to 3704 m/s at 20%.
- The Sideband Peak Count Index (SPCI) captured these transitions effectively, rising from 1.00 for the control specimen to 1.42 for 10% rubber and subsequently declining to 0.98 for 20% rubber, indicating a shift from damage-dominated scattering to improved connectivity.
- Hardened density decreased monotonically with increasing rubber content, from 2274.7 kg/m³ in the control to 2170.7 kg/m³ at 20% replacement, representing a 4.6% reduction while remaining within the normal-weight classification.
- Taken together, the results suggest that replacement levels between 15% and 20% offer an optimal balance between sustainability benefits and functional performance. Although compressive strength and UPV remain significantly below control values, the SPCI values for these specimens are close to that of the control specimen because the observed transition toward quasi-ductile behavior, maintained the structural integrity. Reduced density for these specimens support the feasibility of rubber-modified mortar in pavement applications.
- For non-structural elements such as sidewalks, bike lanes, and pedestrian plazas, rubber replacement up to 20% provides tangible advantages including lower dead loads, improved crack resistance, and enhanced energy dissipation. For semi-structural applications subjected to moderate loads, such as lightly trafficked parking decks or access roads, replacement levels of 10–15% represent a more conservative and reliable range.
- This study also underscores the utility of combining UPV and SPCI as complementary non-destructive evaluation tools for quality control and performance monitoring in the field. Future investigations should focus on surface treatment of rubber particles, assessment of long-term durability under environmental exposures such as freeze–thaw cycles, and validation through full-scale pavement trials. Hence, more research is warranted to expand the understanding of rubber-modified cementitious systems in the following areas:
  - long-term durability assessments under environmental exposures such as freeze–thaw, wetting–drying, and chloride ingress.
  - optimization of particle size gradation and surface treatment strategies to improve interfacial bonding and hydration efficiency.
  - integration of supplementary cementitious materials or nanomaterials to compensate for strength losses; and
  - advanced multi-scale modeling and acoustic simulation studies could also help establish predictive frameworks linking microstructural features with non-destructive indicators, enabling performance-based design of sustainable rubberized concretes.

5. AUTHOR CONTRIBUTIONS: CREDIT

Shruti Singh: Conceptualization, Methodology, Investigation, Data curation, Formal analysis, Writing – original draft. Hee Jeong Kim: Supervision, Resources, Project administration, Writing – review & editing. Tribikram Kundu: Supervision, Resources, Project administration, Writing – review & editing.

6. FUNDING

During this investigation the first author was partially supported by the National Science Foundation's Science and Technology Center - New Frontiers of Sound (NewFoS) through NSF cooperative agreement # 2242925.

7. REFERENCE

[1] Mayer, P., Moran, K., Miller, E., Brander, S., Harper, S., Garcia-Jaramillo, M., Carrasco-Navarro, V., Ho, K., Burgess, R., Thornton Hampton, L., Granek, E., McCauley, M., McIntyre, J., Kolodziej, E., Hu, X., Williams, A., Beckingham, B., Jackson, M., Smith, R., Fender, C., King, G., Bollman, M., Kaushal, S., Cunningham, B., Hutton, S., Lang, J., Goss, H., Siddiqui, S., Sutton, R., Lin, D., & Mendez, M. (2024). Where the rubber meets the road: Emerging environmental impacts of tire wear particles and their chemical cocktails. Science of the Total Environment, 927, 171153.

[2] Hashamfirooz, M., Dehghani, M. H., Khanizadeh, M., Aghaei, M., Bashardoost, P., Hassanvand, M. S., Hassanabadi, M., & Momeniha, F. (2025). A systematic review of the environmental and health effects of waste tires recycling. Heliyon, 11(2), e41909. https://doi.org/10.1016/j.heliyon.2025.e41909

[3] Scott, A. (2023, May 26). Can tires turn green? Chemical & Engineering News. https://cen.acs.org/environment/sustainable-tire-market/101/i17

[4] Algaifi, H. A., Syamsir, A., Baharom, S., Alrshoudi, F., Qaid, A., Al-Fakih, A. M., Mhaya, A. M., & Salah, H. A. (2024). Assessment of acoustic and mechanical properties in modified rubberized concrete. Case Studies in Construction Materials, 20, e03063. https://doi.org/10.1016/j.cscm.2024.e03063

[5] Holmes, N., Browne, A., & Montague, C. (2014). Acoustic properties of concrete panels with crumb rubber as a fine aggregate replacement. Construction and Building Materials, 73, 195–204. https://doi.org/10.1016/j.conbuildmat.2014.09.107

[6] Hunagund, V. N., Naik, H. H., Kambar, B. R., & Bhushan, G. S. (2022). Studies on use of crumb rubber in concrete for acoustical insulation purposes (Project Reference No. 45S_BE_4390). B.V.V. Sangha's Basaveshwar Engineering College, Department of Civil Engineering, Bagalkot. 45th Series Student Project Programme (SPP) – 2021–22.

[7] Fediuk, R., Amran, M., Vatin, N., Vasilev, Y., Lesovik, V., & Ozbakkaloglu, T. (2021). Acoustic properties of innovative concretes: A review. Materials, 14(2), 398. https://doi.org/10.3390/ma14020398

[8] Ocholi, A., Ejeh, S. P., & Yinka, S. M. (2014). An investigation into the thermal performance of rubber-concrete. Academic Journal of Interdisciplinary Studies, 3(5), 29–36. https://doi.org/10.5901/ajis.2014.v3n5p29

[9] Ghedan, R. H., & Hamza, D. M. (2011). Effect of rubber treatment on compressive strength and thermal conductivity of modified rubberized concrete. Journal of Engineering and Development, 15(4), 21–30

[10] Kevin, B., Sarker, P. K., & Madhavan, M. K. (2025). Performance assessment and microstructural characterization of combined surface, chemical, and polymer treated crumb rubber concrete. Scientific Reports, 15, 15853. https://doi.org/10.1038/s41598-025-97189-8

[11] Hoy Menglim, H., Horpibulsuk, S., Chinkulkijniwat, A., Suddeepong, A., Buritatum, A., Yaowarat, T., Choenklang, P., Udomchai, A., & Kantatham, K. (2024). Innovations in recycled construction materials: Paving the way towards sustainable road infrastructure. Frontiers in Built Environment, 10. https://doi.org/10.3389/fbuil.2024.1449970

[12] Noor Azline, M. N., Nabilah, A. B., Nor Azizi, S., & Farah Nora Aznieta, A. A. (2022). A comparative investigation on mechanical strength of blended concrete with surface modified rubber by chemical and non-chemical approaches. Case Studies in Construction Materials, 17, e01444. https://doi.org/10.1016/j.cscm.2022.e01444

[13] Abdulkadir, S. B., Chen, Q., Yilmaz, E., & Wang, D. (2025). Comparative and meta-analysis evaluation of non-destructive testing methods for strength assessment of cemented paste backfill: Implications for sustainable pavement and concrete materials. Materials, 18(12), 2888. https://doi.org/10.3390/ma18122888

[14] Umar, T., Yousaf, M., Akbar, M., Abbas, N., Hussain, Z., & Ansari, W. S. (2022). An experimental study on non-destructive evaluation of the mechanical characteristics of a sustainable concrete incorporating industrial waste. Materials, 15(20), 7346. https://doi.org/10.3390/ma15207346

[15] Sagar, R. V., Roy, T. P., & Kundu, T. (2025). Damage growth monitoring in cementitious materials by nonlinear ultrasonic and acoustic emission techniques. ASME Journal of Nondestructive Evaluation, 8(1), 011008. https://doi.org/10.1115/1.4066197

[16] Basu, S., Thirumalaiselvi, A., Sasmal, S., & Kundu, T. (2021). Nonlinear ultrasonics-based technique for monitoring damage progression in reinforced concrete structures. Ultrasonics, 115, 106472. https://doi.org/10.1016/j.ultras.2021.106472

[17] Shah, A. A., & Ribakov, Y. (2009). Non-linear ultrasonic evaluation of damaged concrete based on higher order harmonic generation. Materials & Design, 30(10), 4095–4102. https://doi.org/10.1016/j.matdes.2009.05.009

[18] Solodov, I., Krohn, N., & Busse, G. (2010). Nonlinear ultrasonic NDT for early defect recognition and imaging. In 10th European Conference on Non-Destructive Testing, Moscow, June 7–11, 2010. https://www.ndt.net/?id=9086

[19] Alnuaimi, H. N., Sasmal, S., Amjad, U., Nikvar-Hassani, A., Zhang, L., & Kundu, T. (2021). Monitoring concrete curing by linear and nonlinear ultrasonic methods. ACI Materials Journal, 118(6), 275–286. https://doi.org/10.14359/51734183

[20] Hu, B., & Kundu, T. (2025). Probabilistic damage analysis of rebar corrosion in recycled aggregate concrete using sideband intensity-based nonlinear ultrasonic technique. Structural Health Monitoring. Advance online publication. https://doi.org/10.1177/14759217251313494

[21] Alnuaimi, H., Amjad, U., Russo, P., Lopresto, V., & Kundu, T. (2021). Monitoring damage in composite plates from crack initiation to macro-crack propagation combining linear and nonlinear ultrasonic techniques. Structural Health Monitoring, 20(1), 139–150. https://doi.org/10.1177/1475921720922922

[22] Sofi, A. (2018). Effect of waste tyre rubber on mechanical and durability properties of concrete–A review. Ain Shams Engineering Journal, 9(4), 2691–2700.

[23] Oikonomou, N., & Mavridou, S. (2009). The use of waste tyre rubber in civil engineering works. In J. M. Khatib (Ed.), Sustainability of construction materials (Chapter 9, pp. 213–238). Woodhead Publishing.

[24] ASTM C1602/C1602M-22. Standard specification for mixing water used in concrete. ASTM International.

[25] ASTM C150/C150M-22. Standard specification for Portland cement. ASTM International.

[26] ASTM C33/C33M-18. Standard specification for concrete aggregates. ASTM International.

[27] ASTM C128-22. Standard test method for density, relative density (specific gravity), and absorption of fine aggregate. ASTM International.

[28] ASTM C566-19. Standard test method for total and organic carbon in water. ASTM International.

[29] ASTM D6270. Standard practice for use of scrap tires in civil engineering applications. ASTM International.

[30] ASTM C305-20. Standard practice for mechanical mixing of hydraulic cement pastes and mortars of plastic consistency. ASTM International.

[31] ASTM C109/C109M-21. Standard test method for compressive strength of hydraulic cement mortars. ASTM International.

[32] ASTM C192/C192M-22. Standard practice for making and curing concrete test specimens in the laboratory. ASTM International.

[33] ASTM C597. Standard test method for pulse velocity through concrete. ASTM International.

[34] He, P. (2004). Simulation of ultrasound pulse propagation in lossy media obeying a frequency power law. IEEE Transactions on Ultrasonics, Ferroelectrics, and Frequency Control, 51(9), 1099–1109.

[35] Krautkrämer, J., & Krautkrämer, H. (2013). Ultrasonic testing of materials (4th ed.). Springer.

[36] ASTM C642. Standard test method for density, absorption, and voids in hardened concrete. ASTM International.

[37] Guo, J., Huang, M., Huang, S., & Wang, S. (2019). An experimental study on mechanical and thermal insulation properties of rubberized concrete including its microstructure. Applied Sciences, 9(14), 2943. *https://doi.org/10.3390/app9142943*

[38] Akinyele, J. O., Salim, R. W., & Kupolati, W. K. (2016). The impact of rubber crumb on the mechanical and chemical properties of concrete. Engineering Structures and Technologies, 74, 197-204. https://doi.org/10.3846/2029882X.2016.1152169